Bioavailability of hydrophobic organic chemicals on an in vitro metabolic degradation using rat liver S9 fraction

Jung-Hwan Kwon[1,*], Hyun-Jeoung Lee[1,2], Beate I. Escher[3,4]

[1]Division of Environmental Science and Ecological Engineering, Korea University, 145 Anam-ro, Seongbuk-gu, Seoul 02841, Republic of Korea

[2]National Institute of Environmental Research, Environmental Research complex, 42 Hwangyeong-ro, Seo-gu, Incheon 22689, Republic of Korea

[3]Department of Cell Toxicology, Helmholtz Centre for Environmental Research – UFZ, Permoserstr. 15, DE-04318 Leipzig, Germany

[4]Environmental Toxicology, Center for Applied Geoscience, Eberhard Karls University Tübingen, Hölderlinstr. 12, DE-72074 Tübingen, Germany

*Corresponding author:

phone: +82 2 3290 3041, e-mail: junghwankwon@korea.ac.kr,

ORCID:

0000-0002-6341-7562 Jung-Hwan Kwon

0000-0002-5304-706X Beate I. Escher

ABSTRACT

Metabolic transformation of highly hydrophobic organic chemicals (HOCs) is one of the most important factors modulating their persistence, bioaccumulation and toxicity. Although sorption of HOCs to cellular matrices affects their bioavailability, it is still not clear how the cellular binding or sorption of HOCs in in vitro metabolism assays influences their enzymatic transformation kinetics. To elucidate effects of non-specific binding to enzymes, we measured apparent enzyme kinetics in an in vitro assay using four polycyclic aromatic hydrocarbons (phenanthrene, anthracene, pyrene and benzo[*a*]pyrene) as model HOCs and S9 mixture isolated from rat liver as a model enzyme mixture. Bovine serum albumin (BSA) was also selected as non-metabolically active protein to investigate effects of protein binding. The observed transformation rates were much higher than those predicted assuming that only freely dissolved HOCs are available for metabolism. A new model including kinetic exchanges between non-specifically bound HOCs and those bound to active enzyme binding sites explained the apparent degradation kinetics at various experimental conditions better. The results are relevant for in vitro-in vivo extrapolation because the metabolic transformation rate in vivo may depend strongly on the local enzyme density and the micro-cellular environment. While non-specific protein binding reduces the unbound fraction of chemicals, this effect could be partially compensated by the facilitated transport to the active sites of the enzymes.

Keywords – enzyme kinetics; facilitated transport; non-specific sorption; equilibrium binding constants; in vitro-in vivo extrapolation (IVIVE)

Introduction

Enzymatic transformation of hydrophobic organic chemicals (HOCs) has been of significant interest because their environmental persistence, bioaccumulation potential, and toxicity strongly depend on their metabolic transformation rate (Cowan-Ellsberry et al. 2008; Lee et al. 2019; Lo et al. 2016; Nichols et al. 2006). The increasing need to evaluate how fast HOCs undergo metabolic transformation cannot be met by in vivo studies because of long experimental time, high experimental cost and ethical concerns. High-throughput in vitro assays are accepted as alternatives to in vivo testing and they come at various levels of complexity to evaluate potential for enzymatic degradation (Austin et al. 2002; Connors et al. 2013; Cowan-Ellsberry et al. 2008; Han et al. 2007; Jones and Houston 2004; Kleinow et al. 1998; Lee et al. 2019; Lo et al. 2015). The simplest method among them is to measure the depletion of a parent chemical in the presence of microsomes or S9 mixture isolated from liver homogenate (Austin et al 2002; Cowan-Ellsberry et al. 2008; Lee et al. 2019).

In an enzymatic assay, the assay medium contains high density of proteins and other cellular materials. It is well-known that hydrophobic chemicals are strongly bound to cellular matrices and this sorption may affect their bioavailability (Austin et al. 2002; Fischer et al. 2019; Gülden and Seibert 2005; Heringa et al. 2004; Hestermann et al 2000; Kwon et al. 2007). Reduced bioavailability of HOCs in such systems is often explained by the equilibrium sorption to medium and non-target sites, which makes them unavailable for the receptors in the test system. For example, Heringa et al. (2004) showed that serum protein concentration strongly influences dose-response relationship in an estrogenicity reporter gene assay and the effect concentrations should be normalized to free concentrations of hydrophobic estrogenic chemicals. Recent studies have confirmed this observation for a wide range of chemicals using a combined modeling and measurement approach (Escher et al. 2019; Fischer et al. 2017; Henneberger et al. 2019). Similarly, Austin and co-workers have shown that metabolic transformation rate is approximately constant

if corrected for the extent of non-specific binding although the apparent transformation rate normalized to protein concentration decreases with increasing enzyme concentration (Austin et al. 2002, 2005). However, their work was limited to mostly ionizable pharmaceuticals of which the logarithms of ionization-corrected distribution ratios between 1-octanol and water at pH 7.4 (log $D_{7.4}$) were lower than 3.0.

On the contrary to the interpretation of decreased transformation rates caused by decrease in freely dissolved concentration, several studies noted that non-specific sorption might accelerate the transport of HOCs to the active target sites (Bittner et al. 2011; Blanchard et al. 2005; Bowman and Benet 2018; Escher et al. 2011; Fujino et al. 2018; Kim et al. 2019; Matsunaga et al. 2019; Miyauchi et al. 2018; Poulin et al. 2016). Non-reactive proteins such as albumin are able to form substrate-albumin complexes and these complexes could deliver the substrate to the active target site. In vitro hepatic clearance rate was measured greater than expected with the decreased freely dissolved concentration in the extracellular medium especially for chemicals that strongly bind to albumin (Blanchard et al. 2005; Bowman and Benet 2018; Kim et al. 2019; Poulin et al. 2016). Escher et al. (2011) compared bioconcentration factor (BCF) of HOCs in fish by extrapolating in vitro metabolic degradation rate obtained using S9 fraction isolated from rainbow trout (*Oncorhynchus mykiss*) with in vivo experimental values. The extrapolated BCF value for hydrophobic nonylphenol assuming that only freely dissolved fraction is available for metabolic degradation was much greater than the experimental BCF-values, suggesting a possibility of delivering nonylphenol non-specifically bound to proteins and other cellular matrices. However, the role of non-specific sorption of HOCs to the bioavailability in metabolic degradation is still not very clear although this is crucial for extrapolating in vitro biodegradation studies to in vivo bioconcentration of highly HOCs.

In this study, we evaluated the effects of non-specific sorption on the apparent enzymatic kinetics in an in vitro metabolic degradation assay using four highly hydrophobic polycyclic aromatic hydrocarbons (PAHs), phenanthrene, anthracene, pyrene and benzo[*a*]pyrene, as model HOCs.

Commercially available S9 mixture isolated from rat liver homogenate was chosen as the model enzyme mixture to provide a proof of principle. Apparent first-order transformation rate constants were measured at various S9 enzyme concentrations, alone and in the presence of various concentrations of bovine serum albumin (BSA). BSA was chosen as non-metabolically active protein in order to investigate effects of non-specific sorption to proteins. In parallel, non-specific binding was measured in form of partition constants between S9 mixture and buffer and between BSA and buffer. A new enzyme kinetics model was proposed to explain the experimental data in this study.

Enzyme kinetic models

Enzymatic degradation of a substrate, *S*, can be described simply by model 1 in Figure 1, where *E* is the enzyme, *E*-*S* is the enzyme-substrate complex after substrate binding to active enzyme sites, *P* is the product, and k_1, k_{-1}, k_2 are kinetic rate constants. Assuming irreversibility of metabolic transformation and pseudo-steady state of the formation of *E*-*S*, a simple rate expression well-known as Michaelis-Menten kinetics is obtained. Equation 1 describes the rate of the total substrate depletion.

$$\text{rate} = -\frac{d[S]_T}{dt} = \frac{k_2[E]_T[S]_T}{\frac{k_{-1}+k_2}{k_1} + [S]_T} = \frac{V_{max}[E]_T[S]_T}{K_m + [S]} \quad (1)$$

where $[E]_T$ is the total concentration of the enzyme (mg L^{-1}), $[S]_T$ is the total substrate concentration (nmol L^{-1}), V_{max} is the maximum velocity (nmol mg^{-1} min^{-1}) and K_m is the half-saturation constant (nmol L^{-1}).

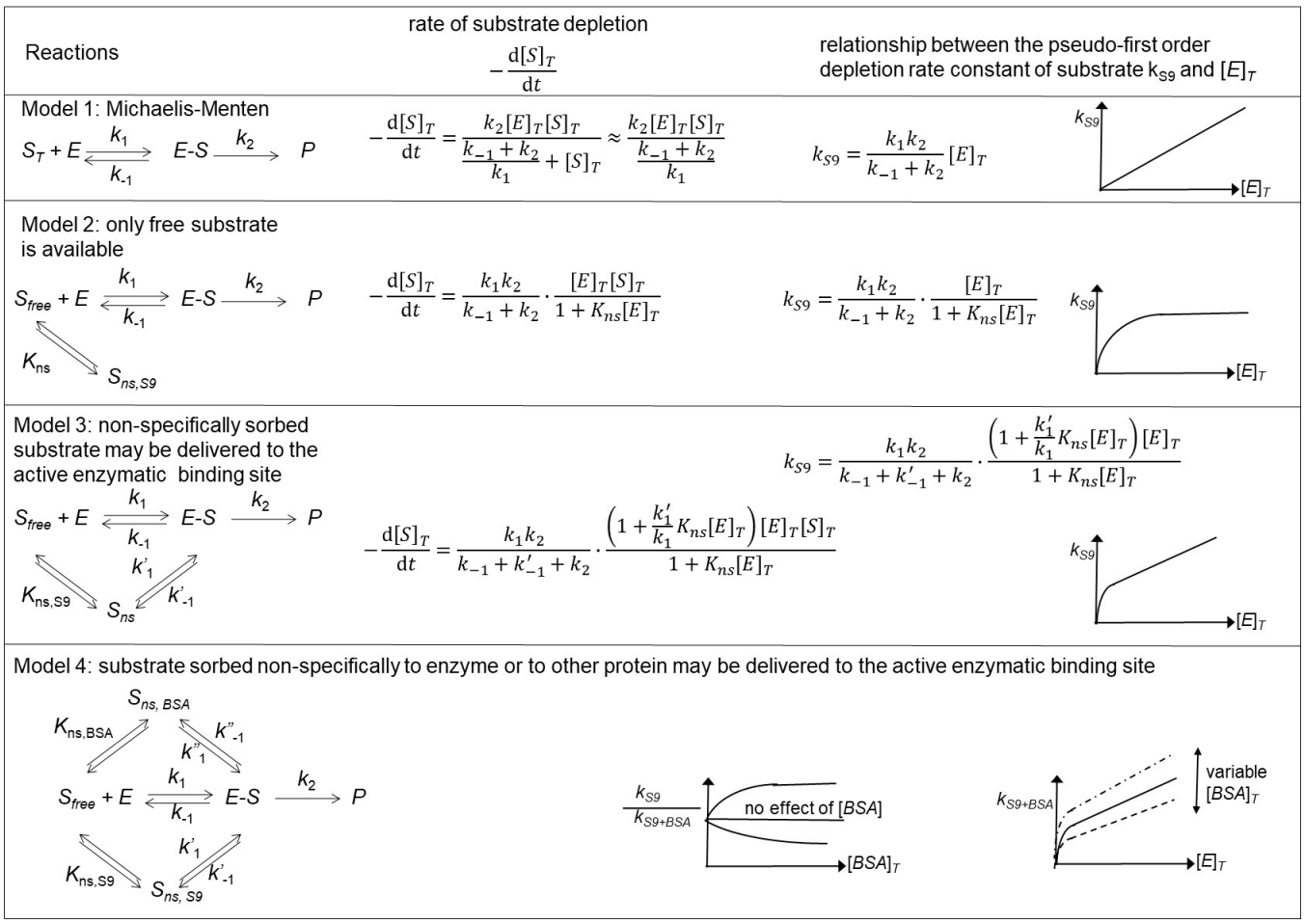

Figure 1. Models describing enzymatic degradation kinetics: model 1, classical Michaelis-Menten model, applicable if the nominal concentration of substrate [S] is available; model 2 applicable if only free substrate $[S]_{free}$ are available; model 3, applicable if non-specifically sorbed substrate $[S]_{ns}$ may be delivered to the active enzymatic binding site; and model 4 applicable if there are other proteins (e.g., BSA) that can sorb substrate and the sorbed substrates may be delivered to the active binding site on S9 protein.

However, for HOCs, a large fraction of the substrate may be bound non-specifically to other protein sites than the active site (Austin et al. 2002; Heringa et al. 2004; Hestermann et al. 2000). Thus, the rate of formation of product is more likely to depend on freely dissolved substrate concentration $[S]_{free}$

than on the total concentration of substrate $[S]_T$ that is spiked in the assay medium due to non-specific binding to experimental matrices. Therefore, we may include non-specific binding in the kinetic model 2 as shown in Figure 1. In general, non-specific sorption of hydrophobic chemicals between water and nano-sized cellular materials are known to be much faster than enzymatic degradation half-life (Cócera et al. 2001; Kraus et al. 2018; Schlautman and Morgan 1993). If we assume that equilibrium is obtained instantaneously, we can model the effects of non-specific sorption using the distribution constant between proteins and the solution. Free substrate concentration, $[S]_{free}$, can be estimated by assuming that $[E\text{-}S]$ is negligible (i.e., $[S]_T \cong [S]_{ns} + [S]_{free}$) compared to free and non-specifically sorbed substrates as:

$$[S]_{free} = \frac{[S]_T}{1 + K_{ns}[E]_T} \quad (2)$$

where K_{ns} is the distribution constant between protein and the buffer solution (L kg^{-1}) via non-specific sorption defined by equation 3.

$$K_{ns} = \frac{[S]_{ns}}{[E]_T[S]_{free}} \quad (3)$$

If total substrate concentration is sufficiently low (eq. 4),

$$\frac{k_{-1} + k_2}{k_1} \gg [S]_T \quad (4)$$

and only free substrates are available for metabolic transformation, equation 1 can be written as:

$$-\frac{d[S]_T}{dt} = \frac{k_1 k_2}{k_{-1} + k_2} \cdot \frac{[E]_T}{1 + K_{ns}[E]_T}[S]_T \quad (5)$$

Thus, the apparent first-order rate constant would be expected to increase linearly with increasing enzyme concentration at sufficiently low $[E]_T$, then approach a constant value as $[E]_T$ increases (eq. 6).

$$k_{S9} = \frac{k_1 k_2}{k_{-1} + k_2} \frac{[E]_T}{1 + K_{ns}[E]_T} \quad (6)$$

If we additionally assume that the non-specifically sorbed substrate can be delivered to the active site on the enzyme (Model 3 in Figure 1), and describe this process with the rate constants, k_1' and k_{-1}',

we obtain a modified rate expression as follows (see Section A, Electronic Supplementary Material for mathematical derivation):

$$-\frac{d[S]}{dt} = \frac{k_1 k_2}{k_{-1} + k_{-1}^{'} + k_2} \cdot \frac{\left(1 + \frac{k_1^{'}}{k_1} K_{ns}[E]_T / 10^6\right)[E]_T}{1 + K_{ns}[E]_T}[S]_T \quad (7)$$

There are two limiting cases of model 3. If the free fraction of substrate dominates (i.e., $K_{ns}[E]_T \ll 1$ and $k_1^{'} K_{ns}[E]_T \ll k_1$) and the substrate concentration is much below the saturation level, equation 7 is simplified to:

$$-\frac{d[S]_T}{dt} = \frac{k_1 k_2 [E]_T}{k_{-1} + k_{-1}^{'} + k_2}[S]_T \quad (8)$$

in which the pseudo-first order rate constant is proportional to the total enzyme concentration. On the other hand, if the bound forms dominate (i.e., $K_{ns}[E]_T \gg 10^6$ and $k_1^{'} K_{ns}[E]_T \gg 10^6 k_1$) and the substrate concentration is low enough, equation 5 is simplified to:

$$-\frac{d[S]_T}{dt} = \frac{k_1^{'} k_2 [E]_T}{k_{-1} + k_{-1}^{'} + k_2}[S]_T \quad (9)$$

Equation 9 is similar to equation 6 except for the slope. The ratio of the slope in equation 8 to that in equation 9 is equal to the ratio of association rate constants (i.e., $k_1$to $k_1^{'}$).

To test if the concept of non-specific sorption is applicable, we can add a second, enzymatically inactive protein, bovine serum albumin (BSA). The reaction model implementing this additional process is depicted in Figure 1 (model 4) but the kinetic equations are not solved.

We measured the transformation rate as a function of substrate concentration for a small number of controls to assure that $[S]_T << K_m$ (See Figure 1, Supplementary Data). Under this condition it is possible to determine a pseudo-first order rate constant of substrate depletion (k_{S9}) which is equivalent to $V_{max}[E]_T/K_m$. Thus plotting k_{S9} versus $[E]_T$ will indicate which kinetic model describes the experimental data best (Figure 1).

Materials and methods

Materials

Four polycyclic aromatic hydrocarbons (PAHs), phenanthrene (CAS RN 85-01-8, 98%, Aldrich, Buchs, Switzerland), anthracene (CAS RN 120-12-7, 99%, Fluka, Buchs, Switzerland), pyrene (CAS RN 129-00-0, 99%, Fluka), and benzo[*a*]pyrene (CAS RN 50-32-8, 99.9%, Supelco, Bellefonte, PA), were chosen as model hydrophobic compounds to evaluate their transformation kinetics in the presence of the enzyme mixture at various non-reactive protein concentrations. Hexachlorobenzene (CAS RN 118-74-1, >99%, Fluka) was used as reference chemical in the sorption experiments because it is hardly degradable. Uninduced rat S9 mixture (Catalog no. RTS9-PL) was purchased from CellzDirect, Inc. (Austin, TX). The protein content of the S9 mixture from the supplier was used. Bovine serum albumin (BSA), dimethylsulfoxide (DMSO), NADP-sodium salts, glucose-6-phosphate, magnesium sulfate, and tris(hydroxymethyl)aminomethyl-chloride (Tris-HCl) were of high purity and purchased from Sigma-Aldrich, Inc. (St. Louis, MO).

Chemical analyses

Concentration of selected PAHs was analyzed using high-performance liquid chromatography system equipped with a P680 HPLC pump and an ASI-100 autosampler (Dionex Softron GmbH, Germering, Germany). They were separated on a C18 Supelcosil LC-PAH column (150 mm × 4.6 mm, 5 μm, Supelco, Bellefonte, PA) at 40°C and detected using an RF-2000 fluorescence detector (Dionex). The excitation wavelength was 275 nm for phenanthrene, 260 nm for anthracene and pyrene, and 290 nm for benzo[*a*]pyrene and the emission wavelengths were 350 for phenanthrene, 420 nm for anthracene and

pyrene, and 430 nm for benzo[*a*]pyrene. De-ionized water and acetonitrile were used as the mobile phase in isocratic mode with the flow rate of 1 mL min^{-1}.

Determination of partition constants and sorption constants

Partition constants between polydimethylsiloxane (PDMS) and 50 mM Tris buffer solution at pH 7.8 ($K_{PDMSbuffer}$) were determined using a dynamic permeation method (Kwon et al. 2007). In short, $K_{PDMSbuffer}$ values were calculated from the apparent permeation rate constant from a PDMS disk loaded with chemicals to a clean PDMS disk separated by the buffer solution, k_d (s^{-1}), using the following relationship:

$$K_{PDMSbuffer} = \frac{D_{buffer} \quad A \quad 1}{\delta_{buffer} V_{PDMS} k_d} \qquad (10)$$

where D_{buffer} is the diffusion coefficient of a chemical in the buffer solution (m^2 s^{-1}), δ_{buffer} is the aqueous boundary layer thickness in the buffer solution (estimated to be 12.5 μm in a previous study; Kwon et al. 2007), A is the surface area of the PDMS disk (m^2), V_{PDMS} is the volume of the PDMS disk (m^3), and k_d is the experimentally measured rate constant (s^{-1}). D_{buffer} was assumed to be equal to the aqueous diffusion coefficient estimated using a correlation with solute's molecular weight (Kwon et al. 2007).

The sorption constants between buffer solution and denatured S9, native BSA or denatured BSA were measured using a PDMS depletion method (Escher et al. 2011; Kwon et al. 2009; Ter Laak et al. 2005). Rat S9 protein and BSA were denatured by increasing the pH of the solution using the equivalent volume of NaOH (yields pH of 14), then immersing the vials for 5 minutes in boiling water, followed by adjusting pH to 9.0 using concentrated HCl. In this way the precipitation of the denatured protein could be avoided.

The detailed procedures of measuring partition constants and sorption constants were described previously (Kwon et al. 2007, 2009). PDMS disks loaded with chemical species were depleted in the

presence of various volumes of deactivated S9 or BSA solution. Partition constants $K_{PDM/Ssus}$ were obtained using a non-linear regression between the fraction lost to the suspension ($C_{PDMS}/C_{PDMS,0}$) and the volume ratio V_{sus}/V_{PDMS} ($m^3_{suspension}$ m^{-3}_{PDMS}):

$$\frac{C_{PDMS}}{C_{PDMS,0}} = \frac{1}{1 + \frac{V_{sus}/V_{PDMS}}{K_{PDMS/sus}}} \tag{11}$$

where C_{PDMS} is the concentration of a chemical in PDMS after equilibrium (mol m^{-3}), $C_{PDMS,0}$ is the initial concentration in PDMS (mol m^{-3}), $K_{PDM/Ssus}$ is the partition constant between PDMS and the suspension containing S9 or BSA ($m^3_{suspension}$ m^{-3}_{PDMS}). Then, the partition constant between protein and buffer ($K_{protein/buffer}$, L kg^{-1}) wss calculated by

$$K_{protein/buffer} = \frac{\frac{K_{PDMS/buffer}}{K_{PDMS/sus}} - 1}{m_{protein}} \tag{12}$$

where $K_{PDMSbuffer}$ is the partition constant between PDMS and buffer and $m_{protein}$ is protein concentration in the suspension (kg L^{-1}). These partition constants were used to quantitatively describe non-specific binding (or sorption) in the metabolic transformation assay.

In vitro metabolic transformation assay

Apparent degradation rate constants were measured at various S9 enzyme concentrations. 8 μL of dimethylsulfoxide containing the test chemical was spiked into an amber vial containing 10 mM NaNADP, 10 mM $MgCl_2$, 40 mM glucose-6-phosphate, and desired concentration of S9 and BSA in 50 mM Tris buffer (pH 7.8) to make a total volume of 1600 μL. The initial concentration of selected PAHs was approximately 100 nM, which is low enough to fall into the linear range of Michaelis-Menten kinetics based on published half-saturation constants of PAHs (Fitzsimmons et al. 2001) and confirmed by the screening experiments in the presented set-up (Figure S1, Electronic Supplementary Material). The

solution was shaken gently (90 rpm) at 25°C in the dark. After pre-determined incubation time (up to 2 h), 200 μL of the solution was taken and immediately mixed with 1800 μL ice-cold acetonitrile to quench the enzymatic transformation. The mixture was then centrifuged at 3,000 g for 10 min to precipitate proteins and the supernatant was taken for chemical analysis. The pseudo-first order degradation rate constant k_{S9} was obtained using linear regression (eq. 11) using concentration measured at six different time points.

$$ln\frac{[S]}{[S_0]} = -k_{S9}t \qquad (13)$$

For a control experiment, changes in concentration of PAHs were also measured in the presence of denatured S9.

Results

Partition constants between S9 and buffer and between BSA and buffer

Table 1 shows all partition and sorption constants obtained in this study and a comparison of the data with octanol-water partition constants (K_{ow}), PDMS-water partition constants (K_{PDMSw}), and liposome-water partition constants (K_{lipw}) using palmitoyl-oleoyl-phosphatidylcholine from literature (Jonker and van der Heijden 2007).

Values of $K_{PDMSbuffer}$ were $10^{3.69}$, $10^{3.82}$, $10^{4.13}$, and $10^{5.01}$ for phenanthrene, anthracene, pyrene, and benzo[*a*]pyrene, respectively, as shown in Table 1 (see Figure S2, Electronic Supplementary Material for experimental determination of the mass transfer kinetics). The values of $K_{PDMS/buffer}$ resulting from a fit of the experimentally measured rate constants were slightly but not statistically significantly smaller than K_{PDMSw} obtained using de-ionized water (Kwon et al. 2007).

Table 1 also shows $K_{S9/buffer}$, $K_{BSA(native)/buffer}$ and $K_{BSA(denatured)/buffer}$ values obtained using equation 12 after determining $K_{PDMSsus}$ using non-linear regression (eq 11) of the fraction remaining in PDMS

($C_{PDMS}/C_{PDMS,0}$) versus volume ratio (see Figure S3, Electronic Supplementary Material). $K_{BSA(native)/buffer}$ and $K_{BSA(denatured)/buffer}$ agreed well, indicating that the assumption is justified that non-specific binding of HOCs to proteins can be regarded as a partitioning process. Control experiments with hexachlorobenzene, which is not metabolizable, also indicated that sorption is not only independent of the tertiary structure of BSA but also independent of the tertiary structure of the S9, because there was no difference between $K_{S9(native)/buffer}$ and $K_{S9(denatured)/buffer}$ (see Figure S4, Electronic Supplementary Material) and pH changes prior and after the denaturation affected the results only slightly. $K_{BSA(native)/buffer}$ values were lower than K_{ow} values by a factor of 14 (pyrene) to 72 (benzo[*a*]pyrene). This difference is in a good agreement with a compilation of data showing that protein-water partition constants are lower than K_{ow} by approximately a factor of 20 (de Bruyn and Gobas 2007).

Table 1. Summary of partition constants between PDMS and Tris-buffer ($K_{PDMS/buffer}$), between S9 and buffer ($K_{S9/buffer}$) and between BSA and buffer ($K_{BSA/buffer}$) with literature log K_{ow}, log K_{PDMSw}, and log K_{lipw}.

	Partition constants						
Chemical	log K_{ow}	log K_{PDMSw}	log K_{lipw}	log $K_{PDMS/buffer}$	log $K_{S9/buffer}$	log $K_{BSA(native)/buffer}$	log $K_{BSA(denatured)/buffer}$
Phenanthrene	4.52[a]	3.87 (3.77, 3.96)[b]	4.86[c], 5.07[d]	3.69 (3.57, 3.78)	4.38 (4.23, 4.49)	3.20 (3.00, 3.33)	3.09 (2.80, 3.33)
Anthracene	4.50[a]	3.98 (3.88, 4.06)[b]	5.15[d]	3.82 (3.72, 3.91)	4.57 (4.43, 4.68)	3.33 (3.21, 3.43)	3.30 (2.98, 3.27)
Pyrene	5.00[a]	4.36 (4.26, 4.45)[b]	5.78[d]	4.13 (3.97, 4.25)	4.87 (4.61, 5.03)	3.85 (3.66, 3.98)	3.59 (3.31, 3.37)
Benzo[*a*]pyrene	6.35[a]	5.09 (4.98, 5.18)[b]	6.98[c], 7.41[d]	5.01 (4.90, 5.09)	5.88 (5.63, 6.04)	4.49 (4.32, 4.61)	4.50 (4.26, 4.65)

Values in parenthesis are the lower and the upper 95% confidence limits calculated using error propagation. [a]Values of log K_{ow} are recommended values in Sangster (1989). [b]Values are from Kwon et al. (2007). [c]Values are from Kwon et al. (2009). [d]Values are from Jonker and van der Heijden (2007) using SPME method.

Effects of enzyme concentration on the metabolic rate

Concentration of PAHs remained unchanged in the presence of denatured S9. The degradation in presence of native S9 followed first-order reaction kinetics with r^2 values mostly higher than 0.9. Figure 2 shows an example of pseudo-first order kinetic decay for benzo[*a*]pyrene at various S9 concentrations. Figure 3 shows the pseudo-first order substrate depletion rate constants k_{S9} (min^{-1}) at various S9 enzyme concentrations for the selected PAHs compiled from at least three different independent experiments. There were detectable rate constants even at very low S9 concentration (0.025 - 0.05 $mg_{protein}$ mL^{-1}). There was a steep increase in the rate constant followed by a gradual linear increase with increasing enzyme concentration. Dashed and solid lines in Figure 3 denote best-fit lines for model 2 and 3 (eq 5 and 7), respectively, using the experimentally measured $K_{S9/buffer}$ values as K_{ns} values.

A linear relationship between the apparent rate constant and the total enzyme concentration would be expected according to the classical Michaelis-Menten kinetics (model 1) and the saturation of the apparent rate constant would expected with increase of the total enzyme concentration according to model 2 but neither model can explain the experimental data. The experimental bi-phasic increase in the apparent rate constant is best explained by model 3 that assumes that non-specifically bound HOCs are also available for enzymatic degradation. The initial steep increase followed by a steady increase in the apparent rate constant indicates that freely dissolved PAHs are more readily available for enzymatic degradation but PAHs non-specifically bound to S9 and cellular matrices are also bioavailable and cannot be neglected although their contribution is slower, so they are not fully available. This means for equation 5 that k_1 is much higher than k_1' but k_1' is sufficiently greater than zero to affect the apparent degradation kinetics.

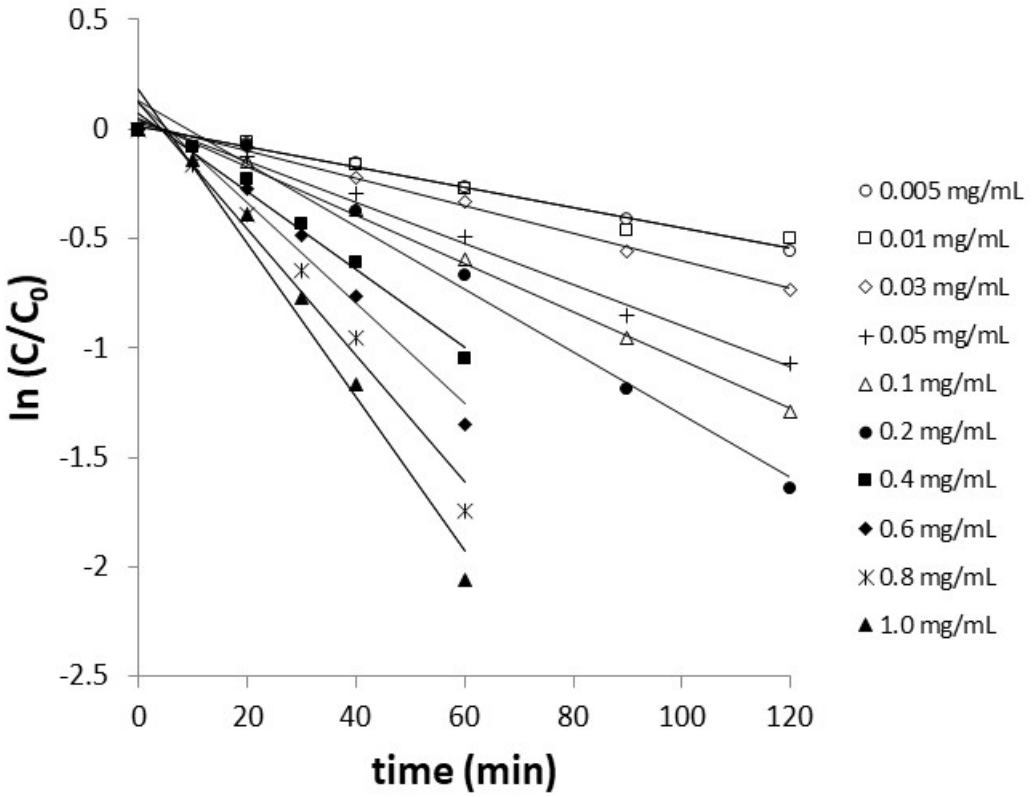

Figure 2. Determination of pseudo-first order rate constant at various S9 concentration for benzo[*a*]pyrene as an example. C and C_0 stand for the total substrate concentration at time t and t=0.

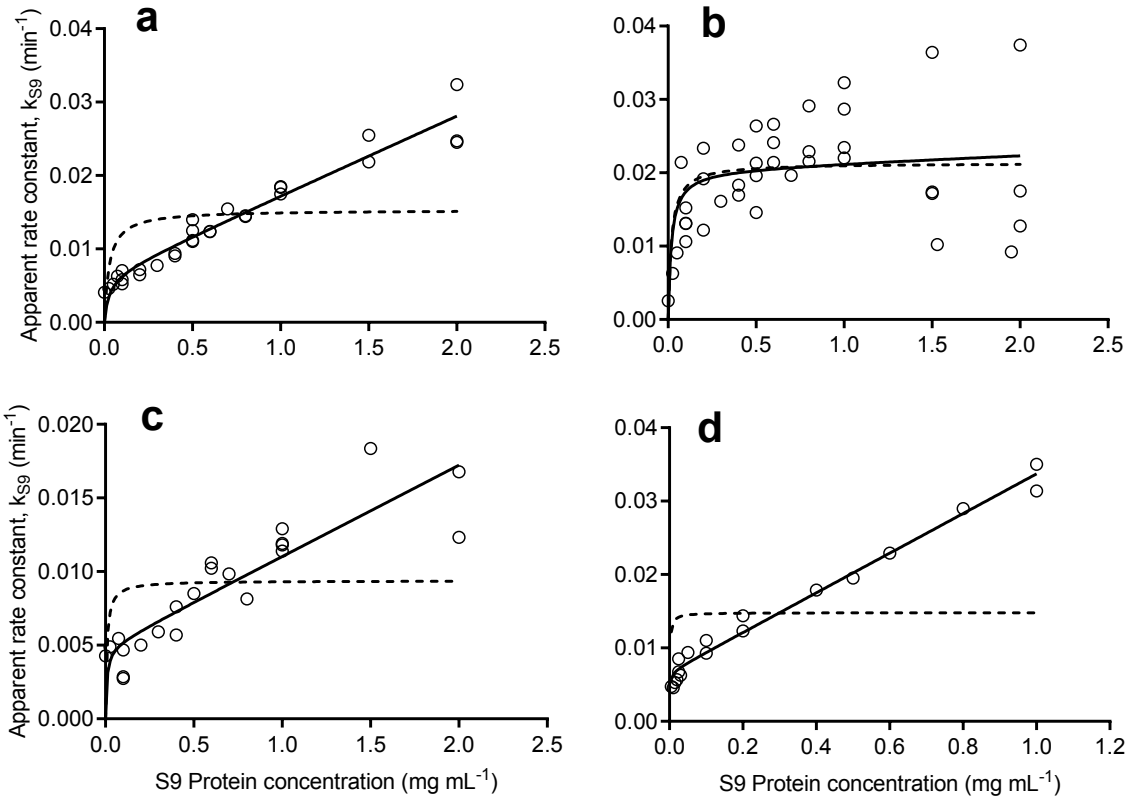

Figure 3. Apparent first-order rate constant k_{S9} at various enzyme concentrations for (a) phenanthrene, (b) anthracene, (c) pyrene, and (d) benzo[*a*]pyrene. The solid lines illustrate the best-fit curves using the new model (equation 7) with the best-fit parameters given in the Electronic Supplementary Material (Table S1). For comparison, the dashed lines show the model that assumed that only free substrates are available (equation 6).

Effects of variable BSA concentrations

We also tested if additional non-specific binding has the same effect as S9 by running experiments with mixtures of 0.5 mg mL^{-1} S9 with different BSA concentrations (0 to 5 mg mL^{-1}). Figure 4 shows apparent first-order rate constants k_{S9+BSA} normalized by the rate constant without BSA, k_{S9}. These ratios k_{S9+BSA}/k_{S9} decreased with increasing BSA for phenanthrene, anthracene, and pyrene (Figure 4a, b, and c). However, the opposite trend was observed for benzo[*a*]pyrene (Figure 4d). Dashed lines refer to predicted ratios k_{S9+BSA}/k_{S9} with using $K_{BSA/buffer}$ and $K_{S9/buffer}$ under the assumption that non-specific

sorption to BSA makes the substrate unavailable for enzymatic degradation and distribution of species in the assay medium is near equilibrium (model 2). The decrease in the freely dissolved concentration by adding BSA to the system satisfactorily explained the decreased apparent rate constants for phenanthrene, anthracene and pyrene although data scattered, whereas this hypothesis fails to explain the experimental data of benzo[*a*]pyrene.

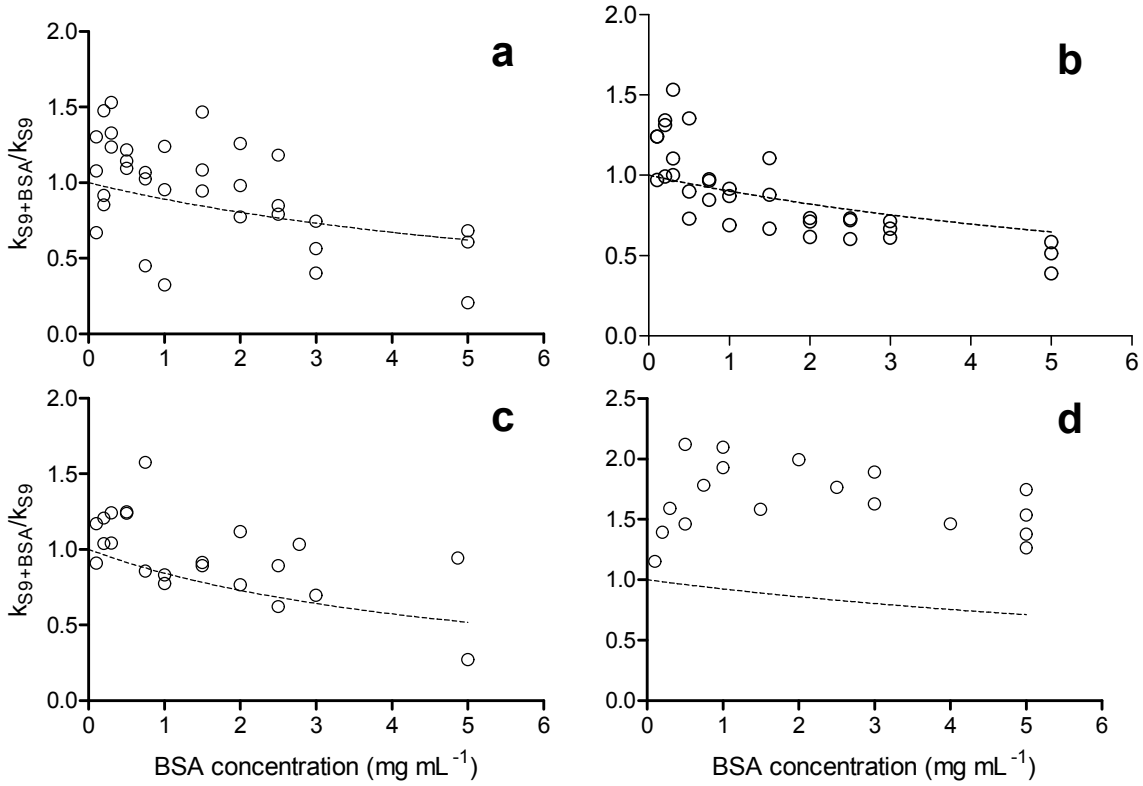

Figure 4. Apparent relative first-order rate constant in the presence of bovine serum albumin k_{S9+BSA}/ k_{S9} for (a) phenanthrene, (b) anthracene, (c) pyrene, and (d) benzo[*a*]pyrene. The concentration of S9 mixture was 0.5 mg mL^{-1}. Dashed lines illustrate expected curves if only free substrate $[S]_{free}$ is available for enzymatic degradation (model 2 in Figure 1).

Discussion

Non-specific sorption of PAHs to S9 and BSA

As summarized in Table 1, $K_{BSA(native)/buffer}$ and $K_{BSA(denatured)/buffer}$ agreed well, indicating that sorption of HOCs to proteins could be regarded as non-specific partitioning. Losing the tertiary structure of the protein through denaturation does not seem to affect the partitioning. Negligible differences between $K_{S9(native)/buffer}$ and $K_{S9(denatured)/buffer}$ for the positive control using non-degradable hexachlorobenzene also supports that this non-specific sorption is independent on the tertiary structure of BSA or S9 and the solution pH (Figure S4). This finding is important because it confirms that the $K_{S9/buffer}$ values, which need to be determined with denatured S9 to differentiate binding from degradation, are representative for native S9. In addition, log $K_{BSA/buffer}$ increased with increasing log K_{ow} (Table 1), suggesting that the affinity of PAHs to albumin is rather unchanged, but the decrease in their aqueous solubility increases log $K_{BSA/buffer}$.

It is also interesting that the experimentally determined $K_{S9/buffer}$ values were higher than $K_{BSA/buffer}$ by approximately one order of magnitude (Table 1). Although protein content of the commercial S9 mixture used in this study was quantified and all results were expressed in relation to protein content of the S9, there was no information on the amount of residual lipids. Liposome-water partition constants (K_{lipw}) of the selected PAHs using palmitoyl-oleoyl-phosphatidylcholine were slightly higher than their K_{ow} values (Jonker and van der Heijden 2007; Kwon et al. 2009) as shown in Table 1. Thus, only 5-10% of residual lipid (w/w) may result in the extraordinarily high sorption constant due to dominating contribution of residual lipids. For comparison, fetal bovine serum contains 2.9 % lipids ($m_{lip}/(m_{lip}+m_{protein})$ (Fischer et al. 2017) and it is conceivable that S9 has a similar lipid content. In contrast the commercially available BSA is purified and fatty acid-free. Although further validation is needed to rationalize the unusually high non-specific sorption to S9 proteins, these sorption constants can be used for the purpose of evaluation of bioavailability of highly HOCs in S9 enzymatic degradation assay.

Comparison of enzyme kinetic models

As shown in Figure 3, the apparent enzymatic degradation rate constants for the four PAHs followed model 3, indicating that HOCs non-specifically sorbed to non-active site of S9 proteins and other organic matter such as proteins and lipids in the medium are still available for enzymatic degradation although they are not as promptly available as freely dissolved forms.

The extension of the proposed kinetic model (model 4 in Figure 1) provides a useful insight for the availability of HOCs to the enzymatic degradation in more complex and thus closer to in vivo conditions. If we assume that substrates non-specifically bound to non-reactive proteins such as BSA are still available for enzymatic activation (i.e., forming [*E*-*S*] complex), we may introduce another association rate constant ($k_1^{''}$) from sorbed to BSA to the active reaction site and dissociation rate constant ($k_{-1}^{''}$) from the active site to sorbed to BSA. If $k_1^{''}$ is negligibly small compared to k_1 or $k_1^{'}$, normalized rate constants would be close to that predicted by the model shown in Figure 4. On the other hand, we may not neglect the effects of $k_1^{''}$ in the overall enzymatic kinetics if $k_1^{''}$ is not negligibly small. The experimental results of benzo[*a*]pyrene can be predicted if $k_1^{''}$ is higher than $k_1^{'}$. Thus, the observed enzymatic degradation kinetics may or may not decrease depending on the chemical investigated and its sorption behavior. Krauss and Goss (2018a, b) proposed in vitro-in vivo extrapolation models including desorption rate constants of HOCs from protein to explain how binding to proteins affect the overall hepatic clearance. Because hepatic metabolism depends on desorption rate constant, fraction bound to proteins, and the intrinsic metabolic rate constant by enzymes (Krause and Goss, 2018b), further investigation on enzymatic kinetics in the presence of various cellular matrices is required.

Implications for environmental bioconcentration of HOCs

Many highly HOCs are suspected to bioconcentrate in aquatic and terrestrial organisms and the key parameter that determines the BCF is in vivo clearance rate (Cowan-Ellsberry et al. 2008; Lee et al. 2019; Nichols et al. 2006). Experimental data in this study clearly showed that not only freely dissolved HOCs are available for metabolic degradation but also HOCs non-specifically bound to serum proteins

or residual lipids are available, providing a clue why experimental BCF values for HOCs are often found to be greater than extrapolated using in vitro enzymatic degradation rate (Escher et al. 2011).

Implications for human quantitative in vitro to in vivo extrapolation models (QIVIVE)

The mechanistic model presented here for in vitro metabolism has also implications for the in vivo situation in human pharmacokinetic models, where it is difficult to estimate the quantitative contribution of non-specificically bound HOCs to be delivered to the active enzymatic sites. Recent studies provided evidence of the facilitated transport of drugs by albumin-mediated uptake mechanisms for the protein bound fraction in hepatocytes and cardiac myocytes (Fujino et al. 2018; Kim et al. 2019; Matsunaga et al. 2019; Poulin et al. 2016). These findings obtained in a cellular environment are consistent with our study in a cell-free environment. Facilitated transport mechanisms warrant further investigations. Since in vitro studies aim at an extrapolation to in vivo, results from in vitro study should be applied for prediction of fate in vivo with great care because the actual metabolic rate in vivo may also depend on local enzyme density and micro-cellular environment. The changes in the apparent degradation rate or the clearance rate should be assessed for more HOCs in the presence of diverse matrices in the microenvironment where the metabolic transformation takes place.

Acknowledgments

Most of experiments of this study was conducted in 2007-2008 at Eawag, Switzerland, and was financially supported by 3R research foundation (3R-Project 100-06). We thank Sibylle Rutishauser (Eawag) for experimental assistance. We are grateful to the HESI Bioaccumulation Project Committee coordinated by Michelle Embry, Annie Weisbrod, Chris Cowan-Ellsberry, and Sue Erhardt for discussions and feedback.

Electronic Supplementary Material

Derivation of rate expressions of enzymatic degradation in the presence of non-specific binding is presented in the Supporting Information. In addition, supplementary raw data is presented (determination of partition constants between PDMS and buffer, BSA and S9, additional partitioning data on hexachlorobenzene, experimental derivation of rate constants).

References

Austin RP, Barton P, Cockroft SL, Wenlock MC, Riley RJ (2002) The influence of nonspecific microsomal binding on apparent intrinsic clearance, and its prediction from physicochemical properties. Drug Metab Dispos 30:1497-1503. https://doi.org/10.1124/dmd.30.12.1497

Austin RP, Barton P, Mohmed S, Riley RJ (2005) The binding of drugs to hepatocytes and its relationship to physicochemical properties. Drug Metab Dispos 33:419-425. https://doi.org/10.1124/dmd.104.002436

Bittner M, Macikova P, Giesy JP, Hilscherova K (2011) Enhancement of AhR-mediated activity of selected pollutants and their mixtures after interaction with dissolved organic matter. Environ Int 37:960-964. https://doi.org/10.1016/j.envint.2011.03.016

Blanchard N, Alexandre E, Abadie C, Lavé T, Heyd B, Mantion G, Jaeck D, Richert L, Coassolo P (2005) Comparison of clearance predictions using primary cultures and suspensions of human hepatocytes. Xenobiotica 35:1-15. https://doi.org/10.1080/00498250400021820

Bowman CM, Benet LZ (2018) An examination of protein binding and protein-facilitated uptake relating to in vitro-in vivo extrapolation. Eur J Pharm Sci 123:502-514. https://doi.org/10.1016/j.ejps.2018.08.008

Cócera M, López O, Estelrich J, Parra JL, de la Maza A (2001) Use of a fluorescence spectroscopy technique to study the adsorption of sodium dodecylsulfonate on liposomes. Chem Phys Lipids 109:29-36. https://doi.org/10.1016/s0009-3084(00)00205-x

Connors KA, Du B, Fitzsimmons PN, Hoffman AD, Chambliss CK, Nichols JW, Brooks BW (2013) Comparative pharmaceutical metabolism by rainbow trout (*Oncorhynchus mykiss*) liver S9 fractions. Environ Toxicol Chem 32:1810-1818. https://doi.org/10.1002/etc.2240

Cowan-Ellsberry CE, Dyer SD, Erhardt S, Bernhard MJ, Roe AL, Dowty ME, Weisbrod AV (2008) Approach for extrapolating in vitro metabolism data to refine bioconcentration factor estimates. Chemosphere 70:1804-1817. https://doi.org/10.1016/j.chemosphere.2007.08.030

de Bruyn AMH, Gobas FAPC (2007) The sorptive capacity of animal protein. Environ Toxicol Chem 26:1803-1808. https://doi.org/10.1897/07-016R.1

Escher BI, Cowan-Ellsberry CE, Dyer S, Embry MR, Erhardt S, Halder M, Kwon J-H, Johanning K, Oosterwijk MTT, Rutishauser S, Segner H, Nichols J (2011) Protein and lipid binding parameters in rainbow trout (Oncorhynchus mykiss) blood and liver fractions to extrapolate from an in vitro metabolic degradation assay to in vivo bioaccumulation potential of hydrophobic organic chemicals. Chem Res Toxicol 24:1134-1143. https://doi.org/10.1021/tx200114y

Escher BI, Glauch L, König M, Mayer P, Schlichting R (2019) Baseline toxicity and volatility cut-off in reporter gene assays used for high-throughput screening. Chem Res Toxicol 32:1646-1655. https://doi.org/10.1021/acs.chemrestox.9b00182

Fischer F, Henneberger L, König M, Bittermann K, Linden L, Goss K-U, Escher B (2017) Modeling exposure in the Tox21 in vitro bioassays. Chem Res Toxicol 30:1197−1208. https://doi.org/10.1021/acs.chemrestox.7b00023

Fischer FC, Henneberger L, Schlichting R, Escher BI (2019) How to improve the dosing of chemicals in high-throughput in vitro mammalian cell assays. Chem Res Toxicol 1462-1468. https://doi.org/10.1021/acs.chemrestox.9b00167

Fitzsimmons PN, Fernandez JD, Hoffman AD, Butterworth BC, Nichols JW (2001) Branchial elimination of superhydrophobic organic compounds by rainbow trout (*Oncorhynchus mykiss*). Aquat Toxicol 55:23-34. https://doi.org/10.1016/s0166-445x(01)00174-6

Fujino R, Hashizume K, Aoyama S, Maeda K, Ito K, Toshimoto K, Lee W, Ninomiya S, Sugiyama Y (2018) Strategies to improve the prediction accuracy of hepatic intrinsic clearance of three antidiabetic drugs: Application of the extended clearance concept and consideration of the effect of albumin on CYP2C metabolism and OATP1B-mediated hepatic uptake. Eur J Pharm Sci 125:181-192. https://doi.org/10.1016/j.ejps.2018.09.021

Gülden M, Seibert H (2005) Impact of bioavailability on the correlation between in vitro cytotoxic and in vivo acute fish toxic concentrations of chemicals. Aquat Toxicol 72:327-337. https://doi.org/10.1016/j.aquatox.2005.02.002

Han X, Nabb DL, Mingoia RT, Yang CH (2007) Determination of xenobiotic intrinsic clearance in freshly isolated hepatocytes from rainbow trout (*Oncorhynchus mykiss*) and rat and its application in bioaccumulation assessment. Environ Sci Technol 41:3269-3276. https://doi.org/10.1021/es0626279

Heringa MB, Schreurs RHMM, Busser F, Van Der Saag PT, Van Der Burg B, Hermens JLM (2004) Toward more useful in vitro toxicity data with measured free concentrations. Environ Sci Technol 38:6263-6270. https://doi.org/10.1021/es049285w

Henneberger L, Mühlenbrink M, König M, Schlichting R, Fischer FC, Escher BI (2019) Quantification of freely dissolved effect concentrations in in vitro cell-based bioassays. Arch Toxicol 93:2295–2305. https://doi.org/10.1007/s00204-019-02498-3

Hestermann EV, Stegeman JJ, Hahn ME (2000) Serum alters the uptake and relative potencies of halogenated aromatic hydrocarbons in cell culture bioassays. Toxicol Sci 53:316-325. https://doi.org/10.1093/toxsci/53.2.316

Jones HM, Houston JB (2004) Substrate depletion approach for determining in vitro metabolic clearance: Time dependencies in hepatocyte and microsomal incubations. Drug Metab Dispos 32:973-982. https://doi.org/10.1124/dmd.104.000125

Jonker MTO, van der Heijden SA (2007) Bioconcentration factor hydrophobicity cutoff: An artificial phenomenon reconstructed. Environ Sci Technol 41:7363-7369. https://doi.org/10.1021/es0709977

Kim S-J, Lee K-R, Miyauchi S, Sugiyama Y (2019) Extrapolation of in vivo hepatic clearance from in vitro uptake clearance by suspended human hepatocytes for anionic drugs with high binding to human albumin: Improvement of in vitro-to-in vivo extrapolation by considering the "albumin-mediated" hepatic uptake mechanism on the basis of the "facilitated-dissociation model". Drug Metab Dispos 47:94-103. https://doi.org/10.1124/dmd.118.083733

Kleinow KM, James MO, Tong Z, Venugopalan CS (1998) Bioavailability and biotransformation of benzo(*a*)pyrene in an isolated perfused in situ catfish intestinal preparation. Environ Health Persp 106:155-166. https://doi.org/10.1289/ehp.98106155

Krause S, Ulrich N, Goss K-U (2018) Desorption kinetics of organic chemicals from albumin. Arch Toxicol 92:1065-1074. https://doi.org/10.1007/s00204-017-2117-4

Krause S, Goss K-U (2018a) In Vitro-in vivo extrapolation of hepatic metabolism for different scenarios - a toolbox. Chem Res Toxicol 31:1195-1202. https://doi.org/10.1021/acs.chemrestox.8b00187

Krause S, Goss K-U (2018b) The impact of desorption kinetics from albumin on hepatic extraction efficiency and hepatic clearance: a model study. Arch Toxicol 92:2175–2182. https://doi.org/10.1007/s00204-018-2224-x

Kwon J-H, Katz LE, Liljestrand HM (2007) Modeling binding equilibrium in a competitive estrogen receptor binding assay. Chemosphere 69:1025-1031. https://doi.org/10.1016/j.chemosphere.2007.04.047

Kwon J-H, Wuethrich T, Mayer P, Escher BI (2007) Dynamic permeation method to determine partition coefficients of highly hydrophobic chemicals between poly(dimethylsiloxane) and water. Anal Chem 79:6816-6822. https://doi.org/10.1021/ac0710073

Kwon J-H, Wuethrich T, Mayer P, Escher BI (2009) Development of a dynamic delivery method for in vitro bioassays. Chemosphere 76:83-90. https://doi.org/10.1016/j.chemosphere.2009.02.023

Lee H-J, Jung J-H, Kwon J-H (2019) Evaluation of the bioaccumulation potential of selected alternative brominated flame retardants in marine fish using in vitro metabolic transformation rates. Sci Total Environ 653:1333-1342. https://doi.org/10.1016/j.scitotenv.2018.10.432

Lo JC, Allard GN, Otton SV, Campbell DA, Gobas FAPC (2015) Concentration dependence of biotransformation in fish liver S9: Optimizing substrate concentrations to estimate hepatic clearance for bioaccumulation assessment. Environ Toxicol Chem 34:2782-2790. https://doi.org/10.1002/etc.3117

Lo JC, Letinski DJ, Parkerton TF, Campbell DA, Gobas FAPC (2016) In vivo biotransformation rates of organic chemicals in fish: Relationship with bioconcentration and biomagnification factors. Environ Sci Technol 50:13299-13308. https://doi.org/10.1021/acs.est.6b03602

Matsunaga N, Ufuk A, Morse BL, Bedwell DW, Bao J, Mohutsky MA, Hillgren KM, Hall SD, Houston JB, Galetin A (2019) Hepatic OATP-mediated clearance in the Beagle dog: assessing in vitro-in vivo relationships and applying cross species empirical scaling factors to improve prediction of human clearance. Drug Metab Dispos 47:215-226. https://doi.org/10.1124/dmd.118.084194

Miyauchi S, Masuda M, Kim SJ, Tanaka Y, Lee KR, Iwakado S, Nemoto M, Sasaki S, Shimono K, Tanaka Y, Sugiyama Y (2018) The phenomenon of albumin-mediated hepatic uptake of organic anion transport polypeptide substrates: Prediction of the in vivo uptake clearance from the in vitro uptake by isolated hepatocytes using a facilitated-dissociation model. Drug Metab Dispos 46:259-267. https://doi.org/10.1124/dmd.117.077115

Nichols JW, Schultz IR, Fitzsimmons PN (2006) In vitro-in vivo extrapolation of quantitative hepatic biotransformation data for fish - I. A review of methods, and strategies for incorporating intrinsic clearance estimates into chemical kinetic models. Aquat Toxicol 78:74-90. https://doi.org/10.1016/j.aquatox.2006.01.017

Poulin P, Burczynski FJ, Haddad S (2016) The role of extracellular binding proteins in the cellular uptake of drugs: Impact on quantitative in vitro-to-in vivo extrapolations of toxicity and efficacy in physiologically based pharmacokinetic-pharmacodynamic research. J Pharm Sci 105:497-508. https://doi.org/10.1002/jps.24571

Sangster J (1989) Octanol-water partition coefficients of simple organic compounds. J Phys Chem Ref Data 18:1111-1228. https://doi.org/10.1063/1.555833

Schlautman MA, Morgan JJ (1993) Effects of aqueous chemistry on the binding of polycyclic aromatic hydrocarbons by dissolved humic materials. Environ Sci Technol 27:961-969. https://doi.org/10.1021/es00042a020

Ter Laak TL, Durjava M, Struijs J, Hermens JLM (2005) Solid phase dosing and sampling technique to determine partition coefficients of hydrophobic chemicals in complex matrixes. Environ Sci Technol 39:3736-3742. https://doi.org/10.1021/es048406p

Declaration of interests

 The authors declare that they have no known competing financial interests or personal relationships that could have appeared to influence the work reported in this paper.

☐The authors declare the following financial interests/personal relationships which may be considered as potential competing interests:

Supplementary Material for

Bioavailability of hydrophobic organic chemicals on an in vitro metabolic degradation using rat liver S9 fraction

Jung-Hwan Kwon[1,*], Hyun-Jeoung Lee[1,2], Beate I. Escher[3,4]
[1]Division of Environmental Science and Ecological Engineering, Korea University, 145 Anam-ro, Seongbuk-gu, Seoul 02841, Republic of Korea
[2]National Institute of Environmental Research, Environmental Research complex, 42 Hwangyeong-ro, Seo-gu, Incheon 22689, Republic of Korea
[3]Department of Cell Toxicology, Helmholtz Centre for Environmental Research – UFZ, Permoserstr. 15, DE-04318 Leipzig, Germany
[4]Environmental Toxicology, Center for Applied Geoscience, Eberhard Karls University Tübingen, Hölderlinstr. 12, DE-72074 Tübingen, Germany

*Corresponding author:
phone: +82 2 3290 3041, e-mail: junghwankwon@korea.ac.kr,

ORCID:
0000-0002-6341-7562 Jung-Hwan Kwon
0000-0002-5304-706X Beate I. Escher

Contents:

A. Mathematical derivations of rate expressions in equation 7

As described in Figure 1 of the main text, non-specific binding of substrate may affect enzymatic degradation kinetics. If we assume that (1) formation of degradation product is irreversible, (2) non-specific binding is very fast and can be considered to be in equilibrium, and (3) concentration of active enzyme-substrate complex is at pseudo-steady state, we can write the differential equations describing the reactions as follows:

$$\frac{d[P]}{dt} = -\frac{d[S]}{dt} = k_2[E-S] \tag{A1}$$

$$\frac{d[E-S]}{dt} = 0 = k_1[S]_{free}[E] + k_1^{'}[S]_{ns}[E] - k_{-1}[E-S] - k_{-1}^{'}[E-S] - k_2[E-S] \tag{A2}$$

Mass balance equations on both enzyme and substrate give

$$[E]_T = [E] + [E-S] \tag{A3}$$

$$[S] = [S]_{free} + [S]_{ns} + [E-S] \cong [S]_{free} + [S]_{ns} \tag{A4}$$

The ratio of non-specifically bound substrate to free substrate can be given by the equilibrium distribution ratio as:

$$K_{ns} = \frac{[S]_{ns}/[E]_T}{[S]_{free}} = \frac{[S]-[S]_{free}}{[E]_T[S]_{free}} \tag{A5}$$

where $[E]_T$ has units of kg L^{-1} and K_{ns} has units of L kg^{-1}. Plugging A3-A5 into A2 and rearranging gives

$$[E-S] = \frac{[E]_T[S]_{free}}{\frac{k_{-1}+k_{-1}^{'}+k_2}{k_1+k_1^{'}K_{ns}[E]_T} + [S]_{free}} \tag{A6}$$

Thus, apparent enzymatic degradation rate becomes

$$-\frac{d[S]}{dt} = \frac{k_2[E]_T[S]_{free}}{\frac{k_{-1}+k_{-1}^{'}+k_2}{k_1+k_1^{'}K_{ns}[E]_T} + [S]_{free}} \tag{A7}$$

Plugging equation 2 of the main text into equation (A7) gives

$$-\frac{d[S]}{dt} = \frac{k_2[E]_T[S]}{\frac{\left(k_{-1} + k_{-1}^{'} + k_2\right)\left(1 + K_{ns}[E]_T\right)}{k_1 + k_1^{'}K_{ns}[E]_T} + [S]} \tag{A8}$$

If the substrate concentration is sufficiently low (eq 7 in main text), one obtains equation 5 in the main text:

$$-\frac{d[S]}{dt} = \frac{k_1 k_2}{k_{-1} + k_{-1}^{'} + k_2} \cdot \frac{\left(1 + \frac{k_1^{'}}{k_1}K_{ns}[E]_T\right)[E]_T}{1 + K_{ns}[E]_T}[S] \tag{7}$$

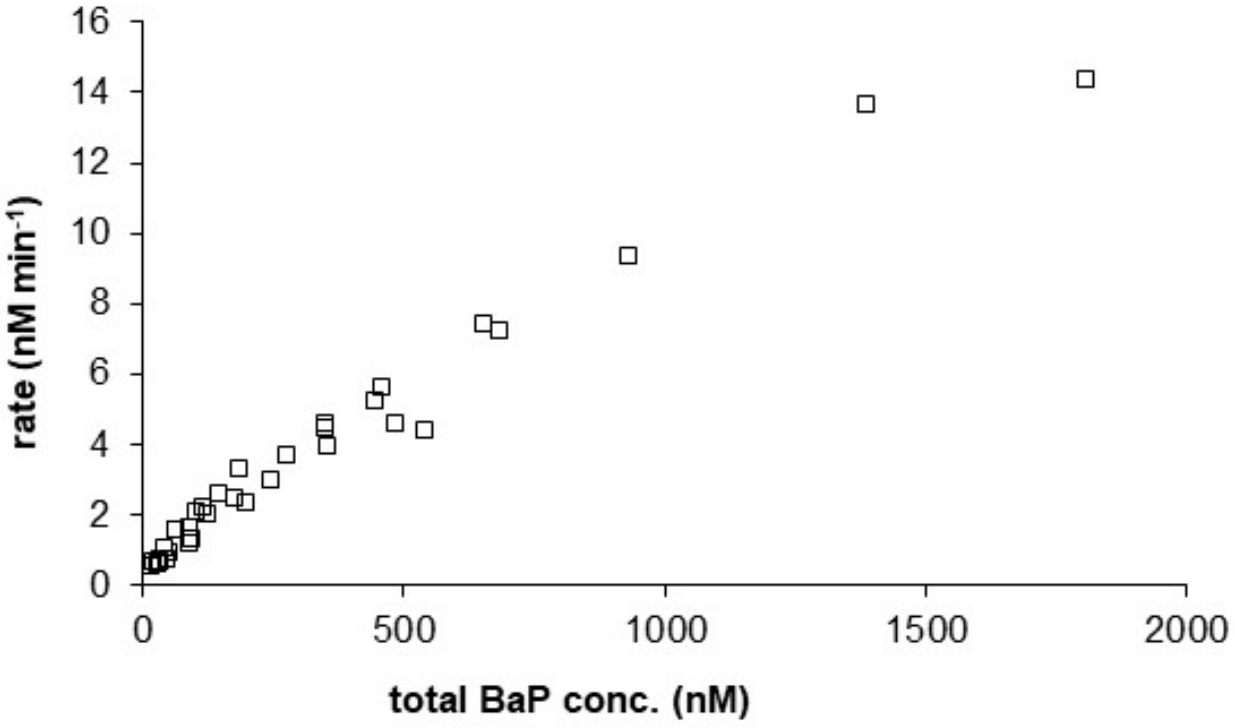

Figure S1. Relationship between degradation rate of benzo[a]pyrene (BaP) in nM min^{-1} and its initial concentration as an example.

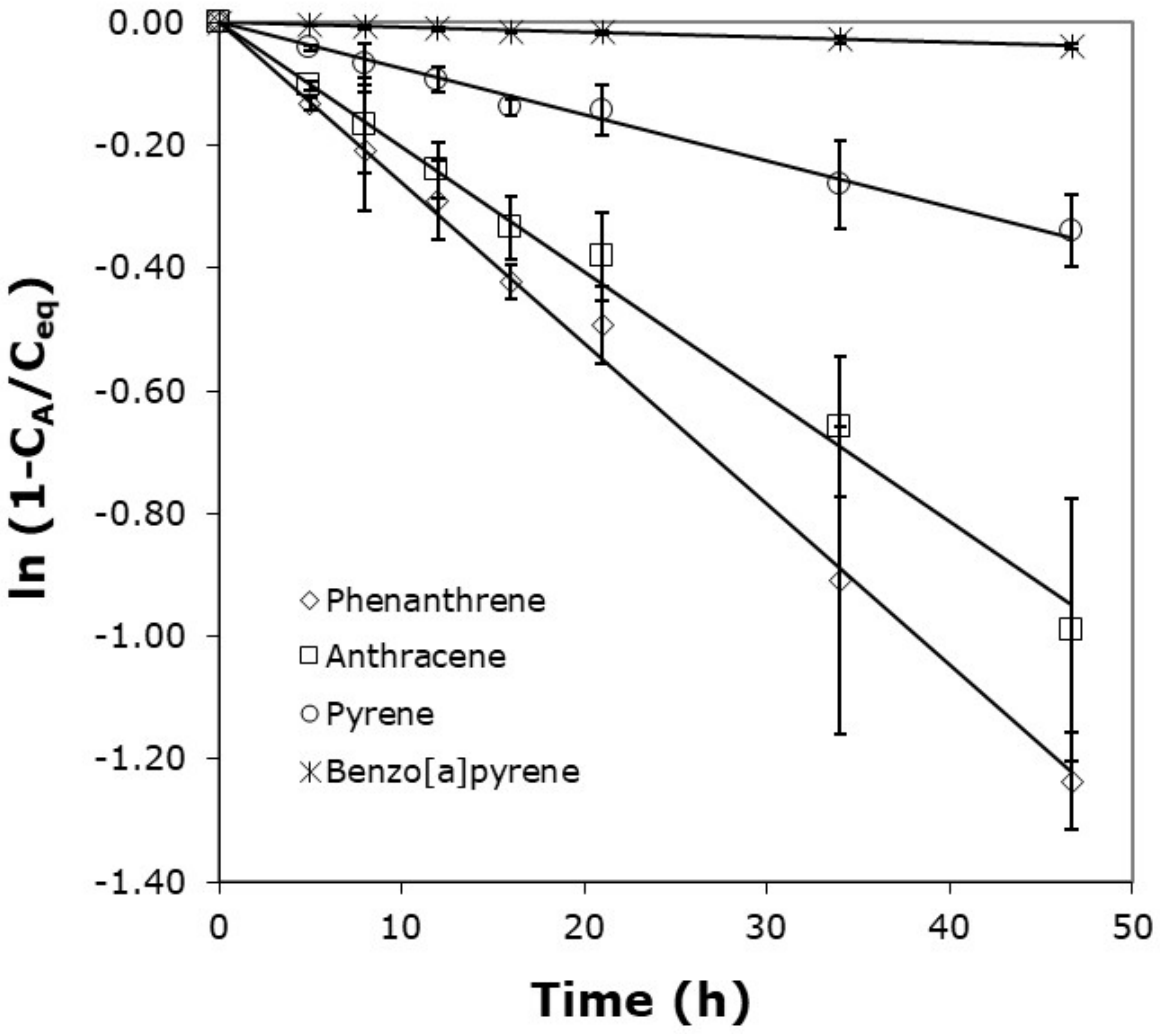

Figure S2. Determination of partition constants between PDMS and the buffer solution ($K_{PDMS/buffer}$) according to Kwon et al. (2007). C_A and C_{eq} present the concentration in the acceptor PDMS and that in equilibrium, respectively. Error bars denote standard deviation of triplicate analysis.

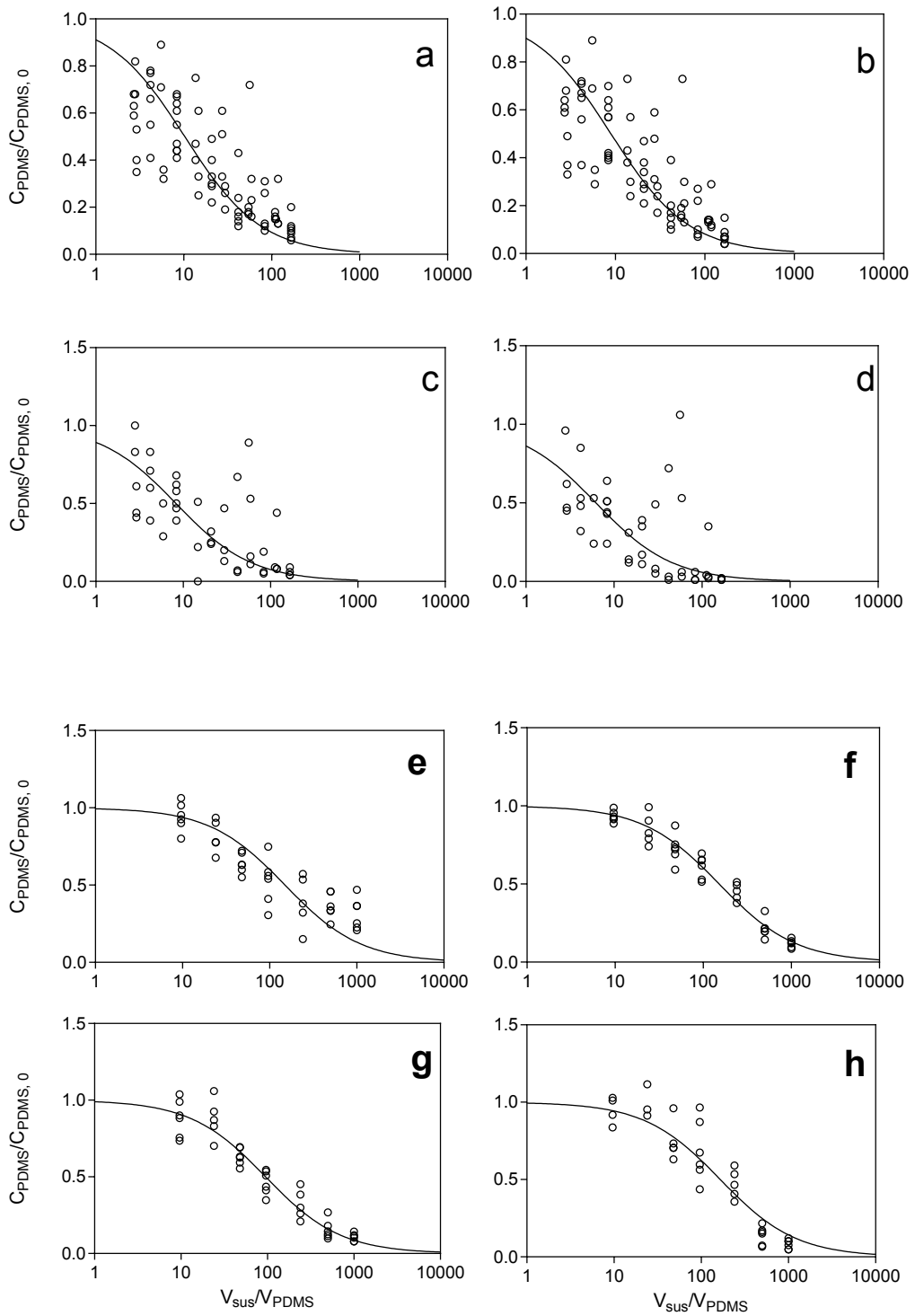

Figure S3. Determination of partition constants $K_{PDMS/sus}$ of (a) phenanthrene, (b) anthracene, (c) pyrene, and (d) benzo[*a*]pyrene between PDMS and deactivated S9 protein suspension and (e) phenanthrene, (f) anthracene, (g) pyrene, and (h) benzo[*a*]pyrene between PDMS and BSA suspension. The lines represent the best fits of the data to equation 9 (main text).

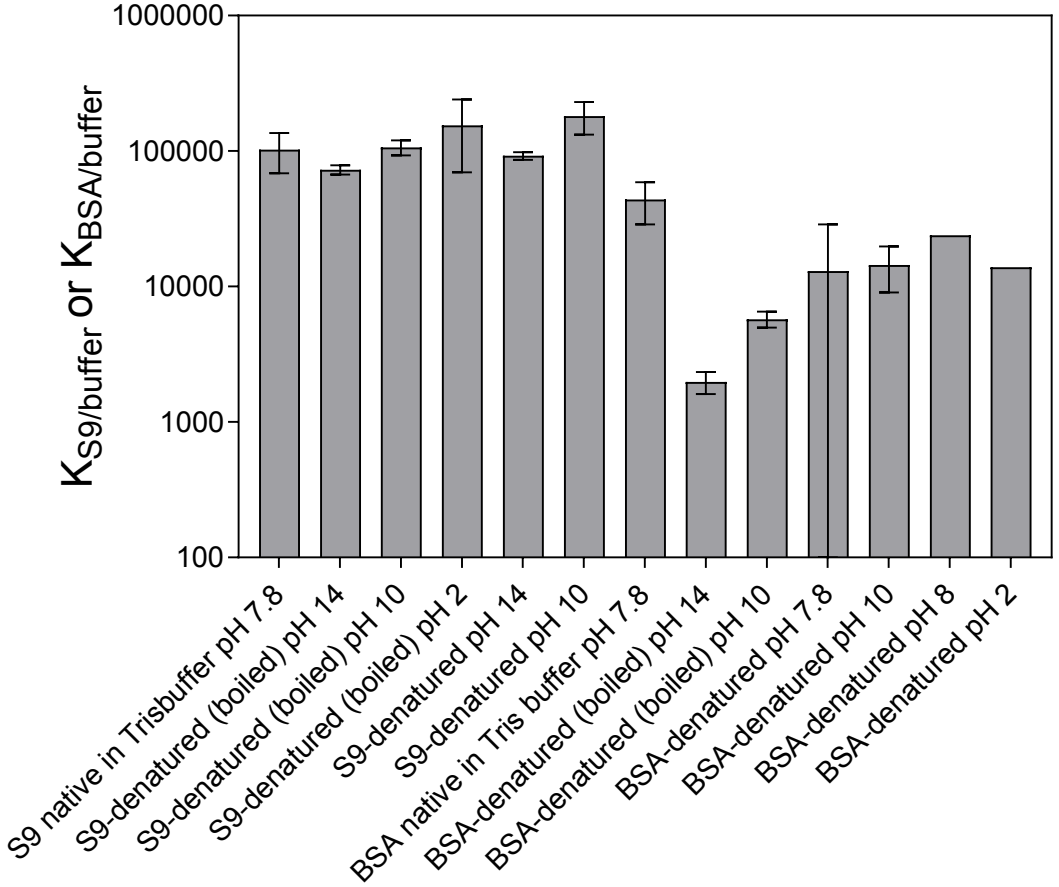

Figure S4. Determination of partition constants $K_{S9/buffer}$ or $K_{BSA/buffer}$ of hexachlorobenzene between S9 protein or BSA suspension and water, in native state or denatured with using various methods, including pH change, pH adjusted to 14 and then boiling for 5 min, and adjustment to various pH-values.

Table S1. Best-fit parameters for apparent first-order rate constants (k_{S9}) using model 2 and 3.

	phenanthrene	anthracene	pyrene	benzo[*a*]pyrene
Model 2				
A $\left(\frac{k_1 k_2}{k_{-1} + k_2}\right)$	0.557(±0.047)	1.142(±0.061)	1.182(±0.115)	13.7(±2.1)
r^2	0.297	0.294	0.119	0.078
Degree of freedom	28	37	21	17
Model 3				
A $\left(\frac{k_1 k_2}{k_{-1} + k'_{-1} + k_2}\right)$	0.247(±0.044)	1.099(±0.104)	0.621(±0.098)	6.27(±0.40)
B $\left(\frac{k'_1}{k_1}\right) \times 10^{-3}$	43.9(±6.4)	0.905(±1.814)	9.96(±2.77)	4.30(±0.39)
r^2	0.938	0.299	0.760	0.982
Degree of freedom	27	36	20	16